



Crossover behavior at an exceptional point for quantum entanglement and correlation in a non-Hermitian XY spin system

Chuanzheng Miao,¹ Yue Li,¹ Jie Wang,² Panpan Zhang,^{1,3} Qinghui Li,¹ Lizhen Hu^{1,3},,^{1,3} Yuliang Xu,¹ and Xiangmu Kong^{1,4,*}

¹*School of Physics and Optoelectronic Engineering, Ludong University, Yantai 264025, China*

²*Naval Aviation University, Yantai 264001, China*

³*Department of Physics, Beijing Normal University, Beijing 100875, China*

⁴*School of Foundational Education, University of Health and Rehabilitation Sciences, Qingdao 266071, China*



(Received 12 November 2023; revised 14 June 2024; accepted 14 June 2024; published 1 July 2024)

Non-Hermitian spin systems have attracted extensive interest due to their unconventional magnetic properties, rich entanglement resources, and unusual quantum criticality phenomena. In this paper, based on the exact solution of a one-dimensional non-Hermitian spin-1/2 XY model with rotation-time-reversal (\mathcal{RT}) symmetry [X. Z. Zhang *et al.*, *Phys. Rev. A* **87**, 012114 (2013)], we study the ground-state energy density, magnetization, correlation functions, quantum entanglement, and correlation in \mathcal{RT} -symmetric and \mathcal{RT} -broken phases as well as their characteristics at the exceptional point. We find that the energy density rises faster with the non-Hermitian parameter $|\gamma|$ in the symmetric region than in the broken one and is elevated rapidly at the exceptional point, and the decay of magnetization has similar results. We analyze the effect of γ on the system and find that the energy density decreases linearly with the external magnetic field h for $\gamma > 0$, while it is bifurcated when $\gamma = 0$. In addition, the behaviors of the energy density indicate that the phase transition caused by symmetry breaking is second order, which is further demonstrated by the magnetization, quantum entanglement, etc. The numerical results of the correlation functions surprisingly indicate that the \mathcal{RT} -broken phase has quasi-long-range order, which is quite different from the Hermitian XY model. Especially, the crossover behavior of the ground-state entanglement shows that it increases with γ in the symmetric region, which is opposite to the case of the broken one, and its maximum always appears at the exceptional point. The above behaviors at the phase boundary are actually ascribed to the fierce competition between γ and h , which results in a rapid decline of magnetization and the appearance of the maximum of entanglement.

DOI: [10.1103/PhysRevB.110.014403](https://doi.org/10.1103/PhysRevB.110.014403)

I. INTRODUCTION

In conventional quantum mechanics, the closed quantum systems are described by Hermitian Hamiltonians. In the last 30 years, there has been a tremendous development in the research of non-Hermitian Hamiltonians [1,2], which can be used to describe systems that couple with the environment, i.e., open systems. In general, the processes that proceed in open systems are dissipative, in which the dynamical behaviors can be described by the master equations (such as the Lindblad form) [2]. The quantum trajectory approach gives a reasonable physical explanation to such dissipative systems; i.e., they evolve under effective non-Hermitian Hamiltonians and are accompanied with quantum jumps which can affect their long-time dynamic evolution [3]. Research indicates that the application of non-Hermitian Hamiltonians is also extensive; for example, they can be used to describe a system that is continuously monitored and a null-measurement outcome is postselected [4–9]. In the above studies, abnormal magnetism caused by a steady-state quantum phase transition is discussed in a non-Hermitian XY model with spontaneous decay [5], and unconventional quantum

criticality is explored by studying the ground state properties of an XXZ model [8]. In 1998 Bender and Boettcher found that non-Hermitian Hamiltonians with parity-time-reversal (\mathcal{PT}) symmetry can still have a full real energy spectrum [10], where \mathcal{P} and \mathcal{T} are parity and time-reversal operators, respectively. These terms have dramatically promoted the development of non-Hermitian physics both theoretically [8,11–18] and experimentally [19–24]. Particularly, they play important roles in describing open systems with balanced gains or losses due to interactions with the environment [2,9,21].

If a Hamiltonian H is commuted with the combined operator \mathcal{PT} , we say that H is \mathcal{PT} symmetric [10]. In experiments, the development of optics provides abundant resources for revealing the concept of \mathcal{PT} symmetry which can be simply achieved by building a gain-loss structure [8,25–27]. In addition to a full real energy spectrum, another remarkable characteristic is the existence of the exceptional point (EP) which separates the symmetric phase from the broken one in the parameter space. In the symmetric phase, the system has a full real energy spectrum and common eigenstates with the combined operator \mathcal{PT} ; i.e., all eigenstates are \mathcal{PT} symmetric. When crossing EP from the symmetric phase to broken one, the imaginary parts of the eigenvalues begin to appear, and thus the corresponding eigenstates become \mathcal{PT} broken even though $[H, \mathcal{PT}] = 0$ [8,10,21]. Along with symmetry

*Contact author: kongxm668@163.com

breaking and the degeneracy of eigenstates at EP, the system exhibits many peculiar properties, in which unusual quantum phase transitions have been studied [8,11–13,28].

As is known to all, quantum entanglement, a unique property of quantum mechanics that describes the indivisibility of subsystems in a composite system, is becoming increasingly significant in various fields [29–33]. Due to its potential applications in quantum teleportation, quantum dense coding, and quantum cryptography, the related studies have currently become quite active [34–37]. In the last two decades, Hermitian quantum many-body spin systems which are employed to study quantum entanglement have become the bridge between quantum information and condensed matter physics [29,38–42]. Especially, the relation between the entanglement and quantum phase transitions has received extensive and sustained attention [40–51]. For non-Hermitian spin systems, the entanglement entropy has recently been investigated, and rich physics phenomena, such as spectral transitions and quantized topological invariants, have been found [14,52–55]. These works provide valuable experience in exploring the entanglement properties of non-Hermitian systems.

In general, it is very difficult to solve a many-body system exactly. For one-dimensional spin systems, their deep connections with Fermi (or Bose) systems provide ingenious methods to solve them exactly [56–58]. The XY model, in particular, gains a great deal of attention in theoretical studies [42,59–64] and is often employed in experiments, in which many interesting phenomena are discovered, such as the order-to-disorder transition in Cs_2CoCl_4 and dimensional reduction in quantum dipolar antiferromagnets [65,66]. For some non-Hermitian spin models, many studies show that they have also been solved exactly, with the corresponding phase diagrams, phase transitions, and quantum information quantities explored [11–14,66–68]. Compared with the optical and mechanical systems, the spin systems have better integration, control, and quantum information storage capabilities; thus the properties such as quantum entanglement and quantum phase transitions, as well as more exotic phenomena in non-Hermitian spin systems, deserve further investigation and discussion.

In 2013, based on \mathcal{PT} -symmetric non-Hermitian quantum theory, Song *et al.* solve exactly a spin model with rotation-time-reversal (\mathcal{RT}) symmetry [69], which has similar properties to the models with \mathcal{PT} symmetry, such as the existence of EP. This model in which the non-Hermitian property comes from the imaginary anisotropic interaction term can be regarded as the complex extension of the one-dimensional quantum anisotropic XY model, and it undoubtedly broadens the exploration of the pseudo-Hermitian field. In recent years, various non-Hermitian models have been studied in optics [21,70–73], cold atoms [74–77], and quantum many-body systems [16,78–81]. These works not only provide a strong theoretical and experimental foundation for studying the concept of \mathcal{RT} symmetry and non-Hermitian phenomena driven by complex interaction, but they also enable the creation of new optical and quantum devices. Besides the \mathcal{RT} symmetry of this model, other properties such as correlation functions and entanglement deserve further study. In this paper, based on the exact solution of the model [5,69,82], we study the phase diagram of the infinite-size system and the

characteristics of ground-state energy density, magnetization, correlation functions, concurrence, and quantum correlation, especially the crossover behaviors of correlation functions and concurrence at EP.

This paper is organized as follows. In Sec. II, we introduce the \mathcal{RT} -symmetric non-Hermitian XY model, and study the phase diagram and ground-state energy in the thermodynamic limit. In Sec. III, we calculate magnetization and correlation functions. Section IV studies the quantum entanglement and discord, along with their crossover behaviors. Section V is the conclusion.

II. MODEL AND PHASE DIAGRAM

Generally, the non-Hermiticity can be realized by introducing the imaginary potential in tightly bound models and adding the imaginary magnetic field in spin models. Meanwhile, the complex coupling between spins can also reflect the non-Hermiticity and similarly imaginary interaction can be achieved in ultracold atomic experiments [8,69]. By analogy to models with \mathcal{PT} symmetry, Song *et al.* study a one-dimensional non-Hermitian spin-1/2 XY model with \mathcal{RT} symmetry [69], in which the Hamiltonian can be written as

$$H = -\frac{J}{2} \sum_{l=1}^N [(1 + i\gamma)\sigma_l^x \sigma_{l+1}^x + (1 - i\gamma)\sigma_l^y \sigma_{l+1}^y] - h \sum_{l=1}^N \sigma_l^z, \quad (1)$$

where σ_l^α ($\alpha = x, y, z$) are the Pauli operators and satisfy the periodic boundary condition $\sigma_l^\alpha = \sigma_{l+N}^\alpha$, and N is the number of spins in this system. J represents the exchange coupling between the nearest-neighbor spins (set $J = 1$), γ is the non-Hermitian anisotropic parameter, h is the external magnetic field, and i the imaginary unit. When $\gamma = 0$, this system reverts to the Hermitian one, and as γ increases, it goes from the \mathcal{RT} -symmetric phase to the broken one.

According to the concept of \mathcal{PT} symmetry, Song *et al.* give the definition of \mathcal{RT} symmetry [69]; i.e., a Hamiltonian is \mathcal{RT} symmetric when it commutes with the combined operator \mathcal{RT} . \mathcal{R} is the rotation operator with the role of counterrotating each spin by $\pi/2$ along the z axis,

$$\mathcal{R} = \exp \left[-i(\pi/4) \sum_{l=1}^N \sigma_l^z \right], \quad (2)$$

and satisfies

$$\mathcal{R} \sigma_l^\alpha \mathcal{R}^{-1} = \begin{cases} \sigma_l^y, & \alpha = x, \\ -\sigma_l^x, & \alpha = y, \\ \sigma_l^z, & \alpha = z, \end{cases} \quad (3)$$

and \mathcal{T} has the function $\mathcal{T}i\mathcal{T}^{-1} = -i$. As a result, one can check that the Hamiltonian of Eq. (1) is \mathcal{RT} symmetric. Besides, if the full spectrums are real, the system is \mathcal{RT} symmetric; when the imaginary part of the eigenvalue appears, \mathcal{RT} symmetry is spontaneously broken.

In order to facilitate the study of the following content, we provide the basic exact solution process of the non-Hermitian Hamiltonian with \mathcal{RT} symmetry [69]. The first step is to map the spin system onto a spinless fermion one by Jordan-Wigner

transformation,

$$\sigma_l^+ = \prod_{j<l} (1 - 2c_j^\dagger c_j) c_l^\dagger \quad (4)$$

and

$$\sigma_l^- = \prod_{j<l} (1 - 2c_j^\dagger c_j) c_l, \quad (5)$$

where $\sigma_l^\pm = \frac{1}{2}(\sigma_l^x \pm i\sigma_l^y)$; c_l^\dagger and c_l are fermionic creation and annihilation operators, respectively. Using the Fourier transformation

$$c_l = \frac{1}{\sqrt{N}} e^{-i\pi/4} \sum_k c_k \exp(ikl) \quad (6)$$

and

$$c_l^\dagger = \frac{1}{\sqrt{N}} e^{i\pi/4} \sum_k c_k^\dagger \exp(-ikl), \quad (7)$$

we map the fermionic Hamiltonian from the coordinate space to the momentum one, in which k is the wave vector, and c_k^\dagger and c_k are fermionic creation and annihilation operators in the momentum space, respectively. Then, the form of Eq. (1) becomes

$$\begin{aligned} H &= 2 \sum_{k>0} [(\cos k + h) c_{-k} c_{-k}^\dagger - (\cos k + h) c_k^\dagger c_k \\ &\quad + i\gamma \sin k c_{-k} c_k + i\gamma \sin k c_k^\dagger c_{-k}^\dagger] \\ &= 2 \sum_{k>0} \left[(c_k^\dagger \ c_{-k}) \begin{pmatrix} -\cos k - h & i\gamma \sin k \\ i\gamma \sin k & \cos k + h \end{pmatrix} \begin{pmatrix} c_k \\ c_{-k}^\dagger \end{pmatrix} \right]. \end{aligned} \quad (8)$$

Finally, using non-Hermitian Bogoliubov transformation

$$\eta_k = u_k c_k + v_k c_{-k}^\dagger \quad (9)$$

and

$$\bar{\eta}_k = u_k c_k^\dagger + v_k c_{-k}, \quad (10)$$

the diagonalized Hamiltonian can be obtained as

$$H = 2 \sum_k \omega_k \bar{\eta}_k \eta_k - \sum_k \omega_k, \quad (11)$$

in which

$$\omega_k = \pm \sqrt{(h + \cos k)^2 - \gamma^2 \sin^2 k}, \quad (12)$$

$k = \frac{2\pi m}{N}$ (the number of fermions $\mathcal{N} = \sum_{l=1}^N c_l^\dagger c_l$ is odd) or $\frac{2\pi(m+1/2)}{N}$ (\mathcal{N} is even), $m = 0, 1, 2, \dots, N-1$, and $k \in (-\pi, \pi]$ ($N \rightarrow \infty$). The new operators $\eta_k, \bar{\eta}_k$ are fermionic operators and satisfy the anticommutation relation, and the concrete forms of u_k and v_k are

$$\begin{aligned} u_k &= \frac{-h - \cos k \pm \sqrt{(h + \cos k)^2 - \gamma^2 \sin^2 k}}{c}, \\ v_k &= \frac{i\gamma \sin k}{c}, \end{aligned} \quad (13)$$

in which c is the normalization constant satisfying $u_k^2 + v_k^2 = 1$.

The vacuum state $|\psi_0\rangle$ that satisfies $\eta_k |\psi_0\rangle = 0$ is given by

$$|\psi_0\rangle = \frac{1}{\sqrt{|u_k|^2 + |v_k|^2}} \prod_{k>0} (u_k - v_k c_k^\dagger c_{-k}^\dagger) |\text{Vac}\rangle, \quad (14)$$

where $|\text{Vac}\rangle$ is the vacuum state of fermion c_l , and the eigenvalue of $|\psi_0\rangle$ is

$$E_0 = - \sum_k \omega_k. \quad (15)$$

The eigenstates of H consist of $|\psi_0\rangle$ and the state $\prod_k \bar{\eta}_k |\psi_0\rangle$, such as $\bar{\eta}_{\pi/3} |\psi_0\rangle$ (with eigenvalue $E_0 + \omega_{\pi/3}$). Generally, a non-Hermitian Hamiltonian has complex eigenvalue, of which the real part represents the energy and the imaginary part describes the rate of decay of the associated eigenstate [7,12]. In the following study, we take the branch where the real part of ω_k is positive, and thus E_0 has the lowest real part and the vacuum state $|\psi_0\rangle$ is the ground state. Although ω_k is imaginary for some values of k (corresponding to the \mathcal{RT} -broken phase), this does not affect the fact that the real part of E_0 remains the lowest.

A. Phase diagram

The phase diagram associated with \mathcal{RT} symmetry for the finite-size system has been studied in Ref. [69]; we then give it a deep discussion and explore it for an infinite-size system. The condition under which the system is \mathcal{RT} symmetric is that the eigenvalues of H are fully real, i.e., $f(k) = (h + \cos k)^2 - \gamma^2 \sin^2 k \geq 0$ for all possible values of k . From this expression, one can get the phase diagrams for different values of N [see Figs. 1(a)–1(c)], in which the shadow regions are \mathcal{RT} symmetric and the blank ones are \mathcal{RT} broken. When N is small, the discontinuity of k causes the phase boundary to be relatively complicated; as N increases, the boundary becomes smooth. In the thermodynamic limit ($N \rightarrow \infty$), the conditions of the phase boundary satisfy [69]

$$f(k) = 0, \quad \frac{\partial f(k)}{\partial k} = 0, \quad (16)$$

from which one can obtain equations of the phase boundary

$$\begin{aligned} h^2 - \gamma^2 &= 1, \quad |h| \geq 1; \\ \gamma &= 0, \quad |h| < 1. \end{aligned} \quad (17)$$

Figure 1(d) is the phase diagram of the infinite-size system, in which the boundary approaches the hyperbola for $|h| \geq 1$, and it also includes the middle segment ($\gamma = 0, |h| < 1$) which corresponds to the Hermitian XX model.

B. Ground-state energy density in \mathcal{RT} -symmetric phase

According to the above discussion, the phase diagram exhibits a unique shape which differs from that of the Hermitian XY model [83]. Ground-state energy density (GSED) is a useful tool for detecting phase transitions; thus we will investigate its variations in both phases and focus on its behavior at the phase boundary. For the sake of simplicity, we first study GSED of a finite-size system (E_0/N) in the \mathcal{RT} -symmetric phase. Figure 2(a) depicts the relation between E_0/N and γ when $h = 1.5$, which shows that E_0/N increases with γ , but

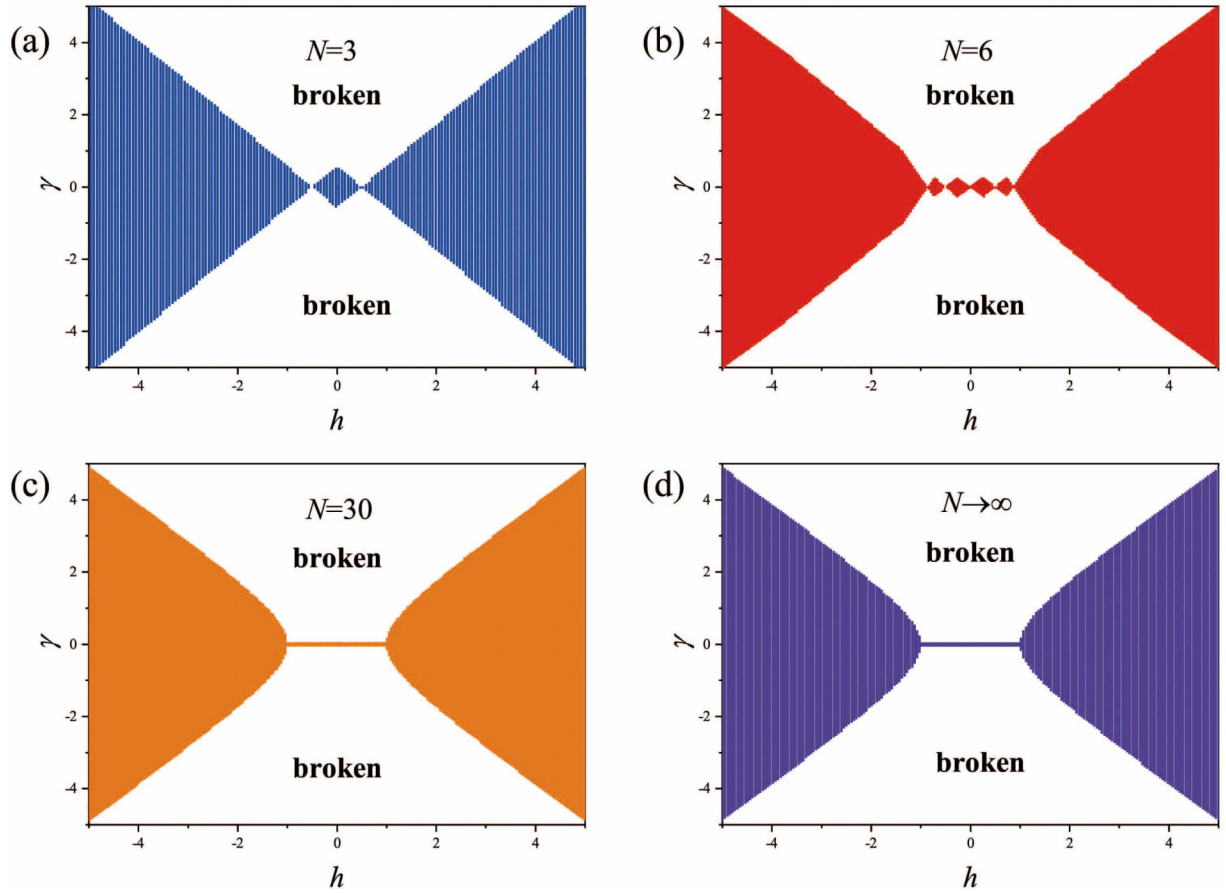


FIG. 1. Phase diagrams in γ - h plane for different values of N . (a), (b), and (c): When N is small, the phase boundary is complicated, and it becomes smoother as N increases. (d) The phase boundary is the hyperbola for $|h| \geq 1$ and the symmetry is also satisfied at the middle segment for $|h| < 1$.

the larger N is, the slower E_0/N increases. In the special case of $\gamma = 0$, from Eqs. (12) and (15), one can get that

$$E_0/N = \left(-\sum_k |h + \cos k| \right) / N, \quad (18)$$

which has two kinds of results for different values of h [see Fig. 2(b)], i.e., $E_0/N = -h$ for $h > 1$, while E_0/N no longer overlaps and begins to bifurcate at $h = 1$. The abnormal behavior of the energy density at $h = 1$ is actually caused by the Ising phase transition ($J = h$) in the general XY model

[84]. When $\gamma > 0$ (non-Hermitian system), E_0/N decreases linearly with h [see Fig. 2(c)], and it tends to be coincident with the increase of N . By fitting the data of $N = 300$, we get the fitted equation $E_0/N = -1.00158h + 0.51627$.

C. Ground-state energy density in the infinite-size system

The GSED in the thermodynamic limit $N \rightarrow \infty$ can be represented as

$$\varepsilon = \lim_{N \rightarrow \infty} \frac{E_0}{N} = \frac{1}{2\pi} \int_{-\pi}^{\pi} \omega_k dk. \quad (19)$$

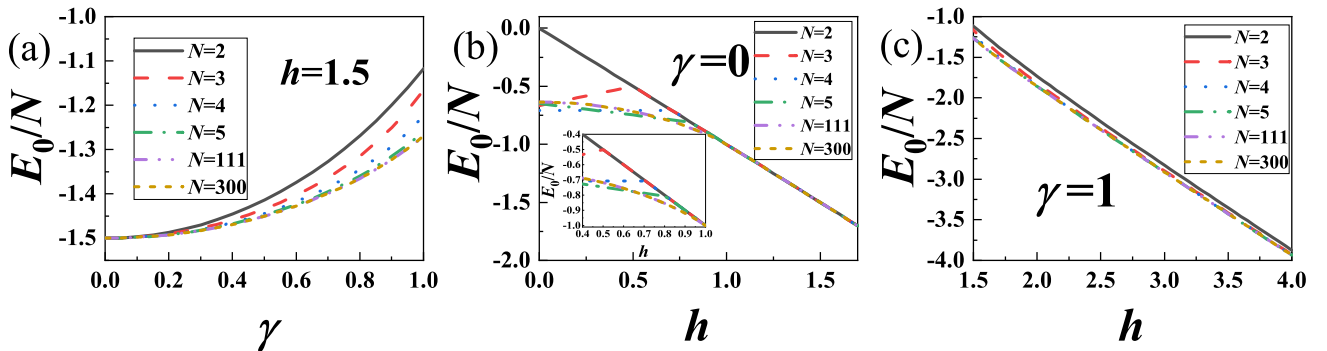


FIG. 2. Ground-state energy density in the \mathcal{RT} -symmetric phase for finite-size system. (a) For different values of N , E_0/N increases with γ at different rates. (b) E_0/N begins to bifurcate as h decreases to 1, while $E_0/N = -h$ when $h \geq 1$. The inset is the variation of E_0/N for $0.4 \leq h \leq 1$. (c) E_0/N varies linearly with h for different values of N , and their slopes are approximately equal.

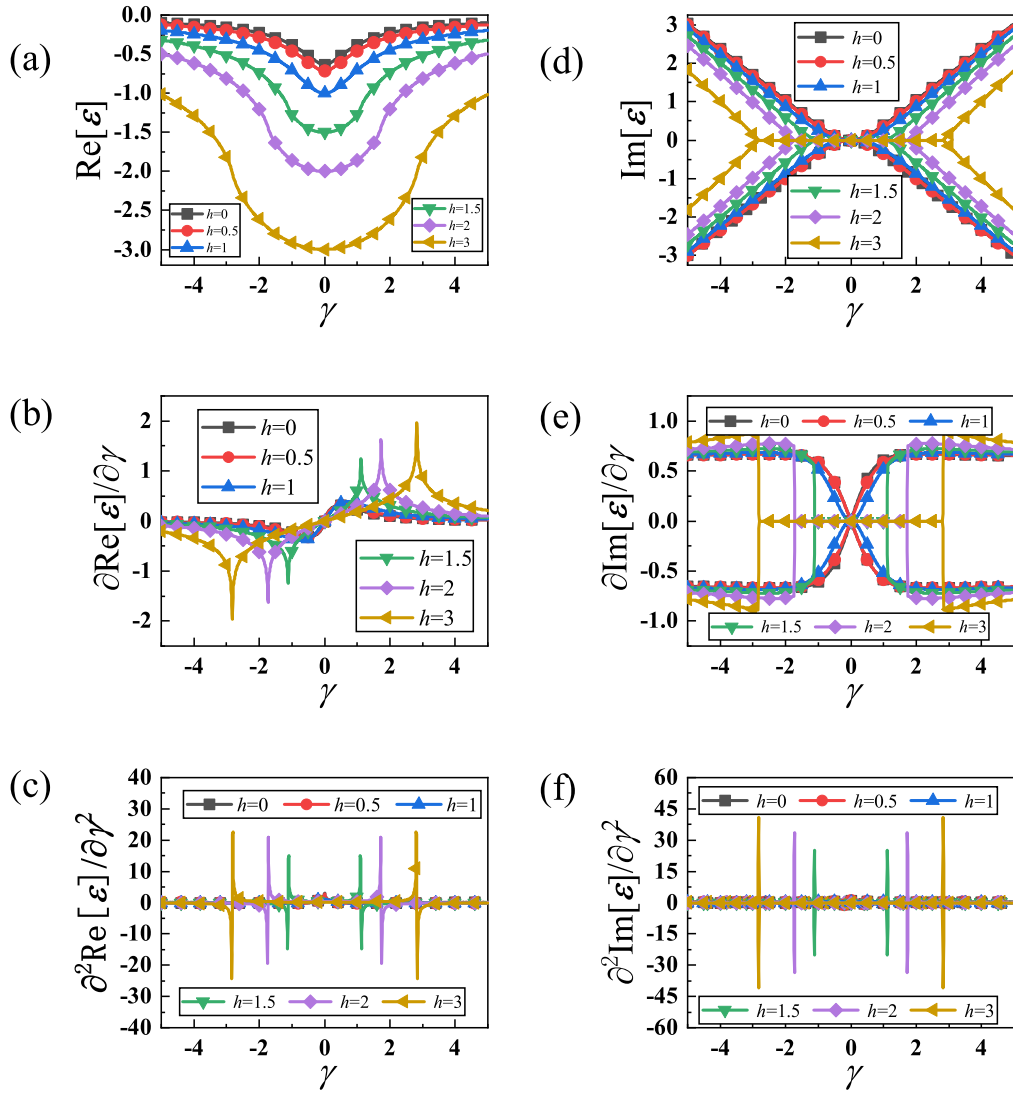


FIG. 3. Real and imaginary parts of GSED as well as their derivatives with respect to γ for $N \rightarrow \infty$. (a) There are inflection points (at EP) on each curve. (b) The derivative of $\text{Re}[\varepsilon]$ has a cusp at EP. (c) The second derivative of $\text{Re}[\varepsilon]$ is discontinuous at EP. (d) $\text{Im}[\varepsilon]$ is complex conjugate in the \mathcal{RT} -broken region, and the larger h is, the wider the range of γ is for $\text{Im}[\varepsilon] = 0$. (e) The first derivative of $\text{Im}[\varepsilon]$ has a jump at EP. (f) The second derivative of $\text{Im}[\varepsilon]$ is also discontinuous at EP.

By numerical integration, its real and imaginary parts as well as their derivatives with respect to γ are obtained, and the results are shown in Fig. 3. We find that $\text{Re}[\varepsilon]$ has a minimum when $\gamma = 0$ for a certain h [see Fig. 3(a)], and it increases faster with $|\gamma|$ in the \mathcal{RT} -symmetric phase than that in the broken one. Besides, $\partial \text{Re}[\varepsilon]/\partial \gamma$ is continuous but has a cusp at EP in Fig. 3(b), which illustrates that $\text{Re}[\varepsilon]$ varies rapidly at EP. For $\text{Im}[\varepsilon]$, it is presented in the form of complex conjugate pairs as shown in Fig. 3(d), and $\partial \text{Im}[\varepsilon]/\partial \gamma$ has a jump at EP [see Fig. 3(e)]; this is because $\text{Im}[\varepsilon]$ is no longer zero when parameters cross EP into the broken phase. In Figs. 3(c) and 3(f), $\partial^2 \text{Re}[\varepsilon]/\partial \gamma^2$ and $\partial^2 \text{Im}[\varepsilon]/\partial \gamma^2$ are discontinuous at EP, indicating that a second-order quantum phase transition occurs simultaneously with symmetry breaking.

To further discuss the effects of γ and h on ε , we give the contour plots of ε . From Fig. 4(a) one can find that ε still has a real part in the \mathcal{RT} -broken phase, because there are some values of k making the real part of ω_k not to be zero.

Meanwhile, $|h|$ can reduce $\text{Re}[\varepsilon]$, which is opposite to the influence of $|\gamma|$, implying that h can weaken the non-Hermitian effect. For $\text{Im}[\varepsilon]$, we just display its negative part in Fig. 4(b), which shows that the effects of $|h|$ and $|\gamma|$ on $|\text{Im}[\varepsilon]|$ are the same as those on $\text{Re}[\varepsilon]$. In Figs. 4(c) and 4(d), the discontinuous behavior of the second derivative of ε can be clearly seen at the dash-dotted line which corresponds to the boundary between the \mathcal{RT} -symmetric phase and the broken one.

III. MAGNETIZATION AND CORRELATION FUNCTION

In this section, we study the magnetization and correlation functions in both \mathcal{RT} -symmetric and \mathcal{RT} -broken phases, and discuss their crossover behaviors at EP.

A. Magnetization

Magnetization is an important concept for studying quantum phase transitions in spin systems, and it can exhibit

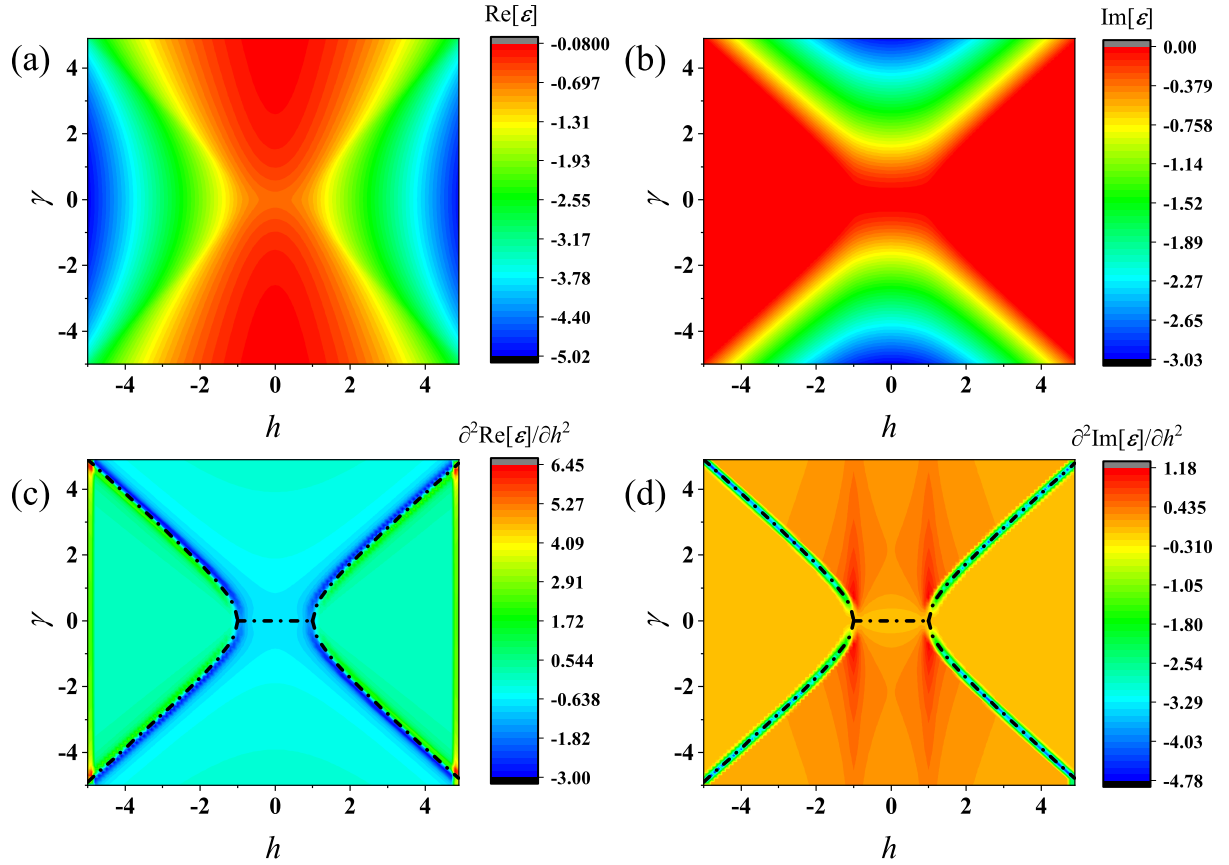


FIG. 4. (a) and (b): Contour plots of the real and imaginary parts of GSED. For a certain h , $\text{Re}[\varepsilon]$ and $|\text{Im}[\varepsilon]|$ have a minimum when $\gamma = 0$, and they increase with $|\gamma|$. (c) and (d): $\partial^2 \text{Re}[\varepsilon]/\partial h^2$ and $\partial^2 \text{Im}[\varepsilon]/\partial h^2$ are discontinuous on the dash-dotted line which is the boundary between \mathcal{RT} -symmetric and \mathcal{RT} -broken phases.

remarkable nonanalytic behavior at the critical point in non-Hermitian spin systems though the number of spins is small [5]. In this subsection, we study it in the infinite-size non-Hermitian system. From Eqs. (4) and (5), one can obtain $\sigma_l^z = 2c_l^\dagger c_l - 1$. Then using Eqs. (9), (10), and (14), the magnetization can be obtained as

$$M = \langle \sigma_l^z \rangle = -\frac{1}{\pi} \int_0^\pi dk \frac{|u_k|^2 - |v_k|^2}{|u_k|^2 + |v_k|^2}. \quad (20)$$

Considering that M is an even function of γ , we only focus on the case of $\gamma \geq 0$. The results of M and its derivatives with respect to γ and h are shown in Fig. 5. In the special case of $\gamma = 0$, we find that M increases with h when $0 < h < 1$; when $h \geq 1$, all spins are magnetized, leading to $M = 1$. In the case of $\gamma > 0$, M is positively correlated with h but negatively correlated with γ . This is because γ enhances the interaction in the x direction, which can reduce the influence of h . The opposite effects of γ and h on M can be seen more clearly from Fig. 5(c). In addition, it is obvious that $\partial M/\partial \gamma$ is nonanalytic at EP [see Fig. 5(b)], indicating that M declines quickly when parameters go from the \mathcal{RT} -symmetric phase to the broken one. Similar phenomena can be seen from Fig. 5(d),

where $\partial M/\partial h$ is also nonanalytic at the phase boundary. The physical mechanism behind these characteristics is the competition between γ and h , and it is extremely intense at the phase boundary.

B. Correlation functions

When discussing critical phenomena, the correlation function is often mentioned. We next study it and its crossover behavior, which is defined as

$$G_\alpha(r) = \langle \sigma_l^\alpha \sigma_{l+r}^\alpha \rangle - \langle \sigma_l^\alpha \rangle \langle \sigma_{l+r}^\alpha \rangle, \quad (21)$$

where r is the distance between spins σ_l and σ_{l+r} . Using Eqs. (4) and (5), one can obtain [56]

$$G_x(r) = \langle B_l A_{l+1} B_{l+1} \cdots A_{l+r-1} B_{l+r-1} A_{l+r} \rangle, \quad (22a)$$

$$G_y(r) = (-1)^r \langle A_l B_{l+1} A_{l+1} \cdots B_{l+r-1} A_{l+r-1} B_{l+r} \rangle, \quad (22b)$$

$$G_z(r) = \langle A_l B_l A_{l+r} B_{l+r} \rangle - \langle \sigma_l^z \rangle \langle \sigma_{l+r}^z \rangle, \quad (22c)$$

in which $A_l = c_l^\dagger + c_l$ and $B_l = c_l^\dagger - c_l$. Due to the existence of h in the z direction, it is more significant to study the correlation function in the x - y plane. By means of Wick's theorem, $G_x(r)$ can be calculated through the Pfaffian of a skew-symmetric matrix [5], i.e.,

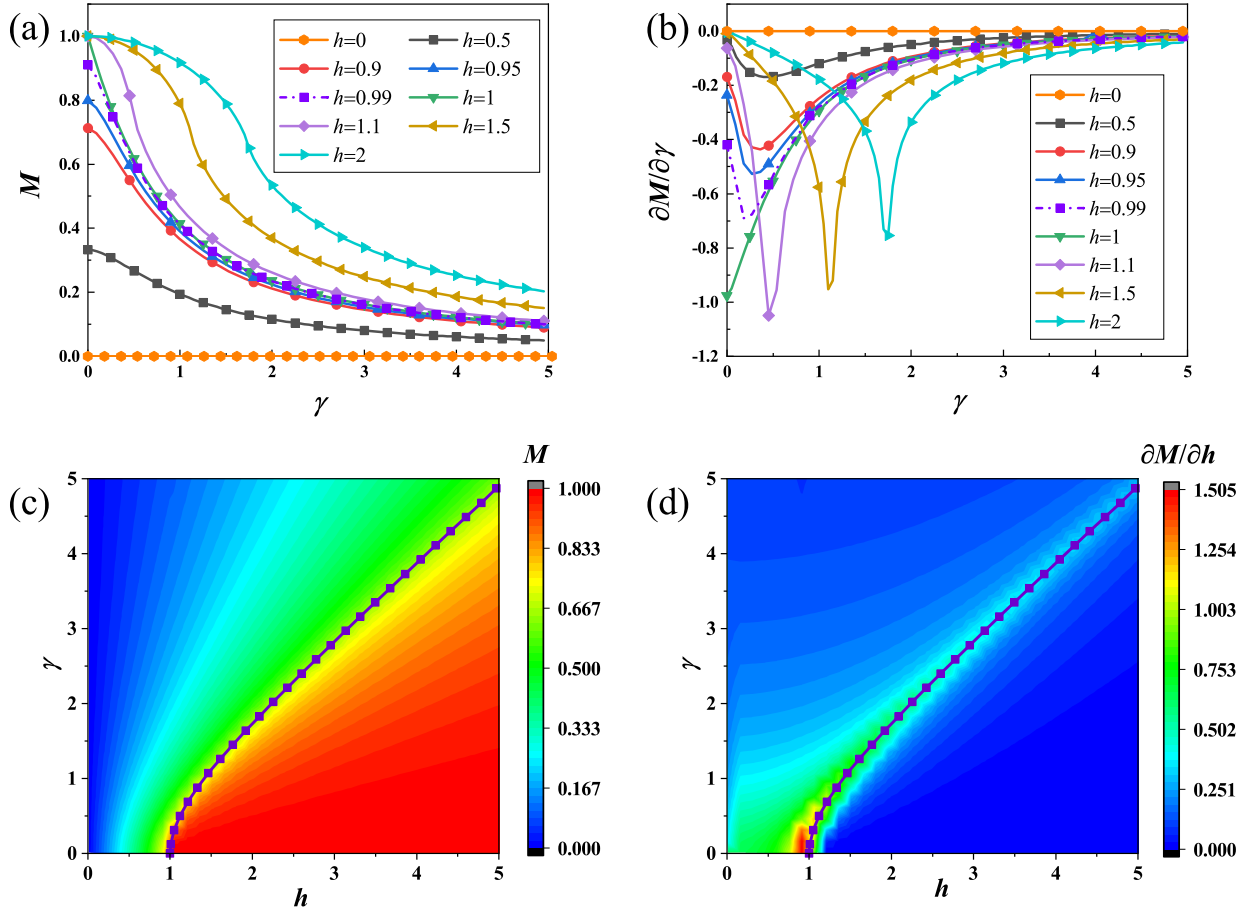


FIG. 5. Magnetization and its derivatives with respect to γ and h . (a) M as a function of γ for different values of h . At $\gamma = 0$, it increases with h for $0 < h < 1$; $M = 1$ (maximum) for $h \geq 1$. (b) $\partial M / \partial \gamma$ varies smoothly with γ when $0 < h \leq 1$, while it has a cusp at EP when $h > 1$. (c) and (d): The solid lines in the contour plots are the boundaries between \mathcal{RT} -symmetric and \mathcal{RT} -broken phases.

$$G_x(r) = \text{Pf} \begin{pmatrix} 0 & \langle B_l B_{l+1} \rangle & \langle B_l B_{l+2} \rangle & \cdots & \langle B_l B_{l+r-1} \rangle & \langle B_l A_{l+1} \rangle & \langle B_l A_{l+2} \rangle & \cdots & \langle B_l A_{l+r} \rangle \\ & 0 & \langle B_{l+1} B_{l+2} \rangle & \cdots & \langle B_{l+1} B_{l+r-1} \rangle & \langle B_{l+1} A_{l+1} \rangle & \langle B_{l+1} A_{l+2} \rangle & \cdots & \langle B_{l+1} A_{l+r} \rangle \\ & & 0 & \cdots & \vdots & \vdots & \vdots & \cdots & \vdots \\ & & & 0 & \langle B_{l+r-2} B_{l+r-1} \rangle & \langle B_{l+r-2} A_{l+1} \rangle & \langle B_{l+r-2} A_{l+2} \rangle & \cdots & \langle B_{l+r-2} A_{l+r} \rangle \\ & & & & 0 & \langle B_{l+r-1} A_{l+1} \rangle & \langle B_{l+r-1} A_{l+2} \rangle & \cdots & \langle B_{l+r-1} A_{l+r} \rangle \\ & & & & & 0 & \langle A_{l+1} A_{l+2} \rangle & \cdots & \langle A_{l+1} A_{l+r} \rangle \\ & & & & & & 0 & \cdots & \vdots \\ & & & & & & & 0 & \langle A_{l+r-1} A_{l+r} \rangle \\ & & & & & & & & 0 \end{pmatrix}, \quad (23)$$

in which the elements on the bottom left are given by the skew symmetry, and the pair contractions of A_l and B_l are

$$\langle A_l A_{l+r} \rangle = \delta_{ll+r} + \frac{1}{\pi} \int_0^\pi dk \frac{u_k v_k^* - u_k^* v_k}{|u_k|^2 + |v_k|^2} \sin(kr), \quad (24a)$$

$$\langle B_l B_{l+r} \rangle = -\delta_{ll+r} + \frac{1}{\pi} \int_0^\pi dk \frac{u_k v_k^* - u_k^* v_k}{|u_k|^2 + |v_k|^2} \sin(kr), \quad (24b)$$

$$\langle A_l B_{l+r} \rangle = -\langle B_{l+r} A_l \rangle = \frac{1}{\pi} \int_0^\pi dk \frac{|u_k|^2 - |v_k|^2}{|u_k|^2 + |v_k|^2} \cos(kr) + \frac{1}{\pi} \int_0^\pi dk \frac{u_k v_k^* + u_k^* v_k}{|u_k|^2 + |v_k|^2} \sin(kr). \quad (24c)$$

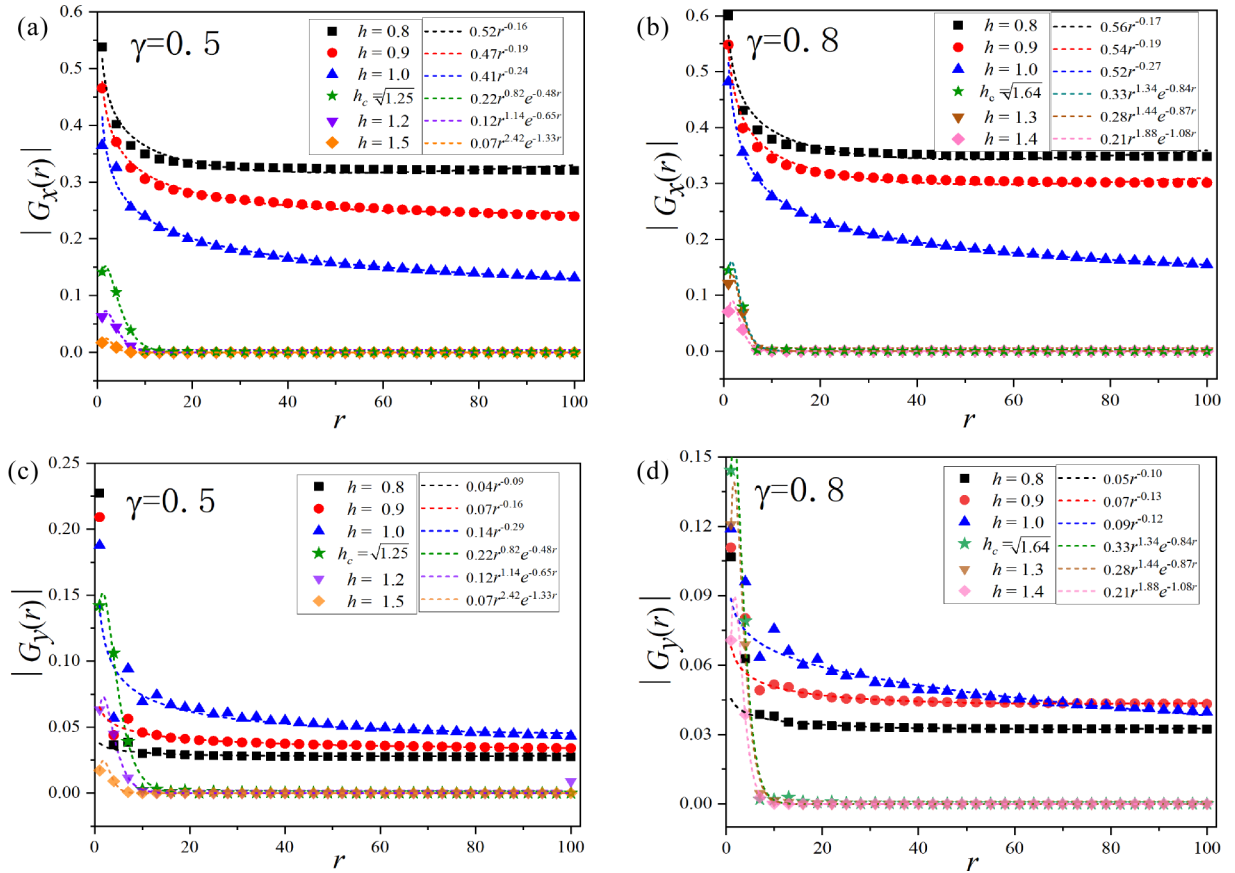


FIG. 6. Correlation function versus r for different values of h . The symbols are numerical results of $|G_\alpha(r)|$ ($\alpha = x, y$) for $\gamma = 0.5$ and 0.8 ; dashed lines are approximately fitting results which satisfy the equation $|G_\alpha(r)| = ar^{-b}e^{-cr}$. h_c is the value at EP when γ is a constant. (a) and (b): $|G_x(r)|$ decays according to a power law as r increases for $h < h_c$; it shows the exponential decay for $h \geq h_c$. (c) and (d): When $h < h_c$, the symbols are dispersed when r is small, but they still fit well as r increases, which shows that $|G_y(r)|$ decays according to a power law. When $h \geq h_c$, $|G_y(r)|$ has the same result as $|G_x(r)|$.

For $G_y(r)$, its calculation process is similar to $G_x(r)$.

Figure 6 shows the variation of correlation functions in the x and y directions with distance r . The symbols in figures are produced by numerical calculation, and dashed lines are fitting results satisfying the equation $G_\alpha(r) = ar^{-b}e^{-cr}$, in which a, b, c are fitting parameters. It is evident that $|G_\alpha(r)|$ will decay exponentially with r when $c > 0$ and according to a power law when $b > 0, c = 0$. We first discuss the characteristics of $|G_x(r)|$ in different phases. The function of $|G_x(r)|$ with r is shown in Figs. 6(a) and 6(b). When $h < h_c$ (broken phase), c almost equals zero, which indicates that $|G_x(r)|$ decays according to a power law and there is quasi-long-range order in the broken phase. Besides, the speed of decay is comparatively enhanced with the increase of h . When $h \geq h_c$ (symmetric phase), it is shown that c is no longer zero, indicating that $|G_x(r)|$ decays exponentially and the short-range order appears. In the case of $|G_y(r)|$, its variation with r is shown in Figs. 6(c) and 6(d). When $h < h_c$, the fitted lines also present the power-law decay; when $h \geq h_c$, due to the preservation of \mathcal{RT} symmetry, its results are the same as $|G_x(r)|$ in Figs. 6(a) and 6(b), respectively, where they exhibit the exponential decay.

The numerical results show that the correlation functions of the non-Hermitian model studied are uncommon. For the Hermitian anisotropic XY model [56], its ground state is

antiferromagnetic which features with long-range order. Only at the anisotropic critical point ($\gamma = 0$), the correlation functions decay according to a power law and quasi-long-range order appears. In the presence of the real magnetic field [83,85], it also exhibits quasi-long-range order when the Ising transition takes place ($\gamma = h$), while short-range order appears in the paramagnetic phase ($\gamma < h$). For the model studied, the emergence of quasi-long-range order in the \mathcal{RT} -broken phase is quite fascinating. It has recently been discovered that quasi-long-range order and the gapless phase of non-Hermitian spin systems are strongly connected [68]. In the \mathcal{RT} -broken phase, one can check that there are always some values of k making the real part of the energy gap ω_k equal to zero, which leads to the emergence of quasi-long-range order. In the \mathcal{RT} -symmetric phase, the order is destroyed by large values of h , resulting in the short-range correlation being similar to that in the paramagnetic phase.

IV. QUANTUM ENTANGLEMENT AND DISCORD

We have investigated the GSED, magnetization, and correlation functions of the model studied and discussed their crossover behaviors. In this section, we study the physical quantities associated with quantum information, such as quantum entanglement and discord.

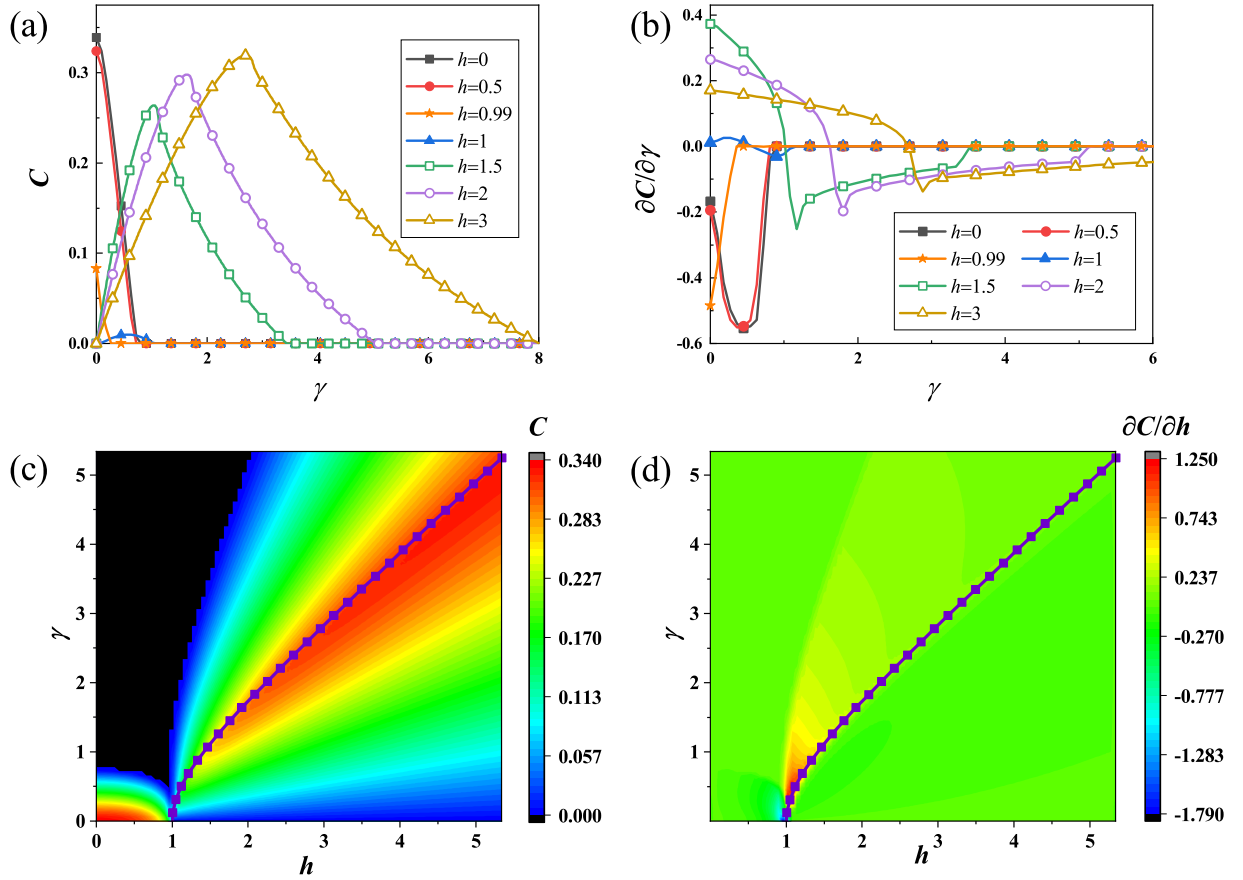


FIG. 7. Concurrence and its derivatives with respect to γ and h . (a) C decreases to zero with γ when $0 < h < 1$, while it has a maximum at EP when $h \geq 1$. (b) $\partial C / \partial \gamma$ is nonanalytic at EP. (c) The variations of C with γ in different phases are opposite, and the maximum of C appears at the phase boundary. (d) $\partial C / \partial h$ is nonanalytic at the phase boundary, especially when γ is small.

A. Ground-state quantum entanglement

Concurrence is an essential measure of quantum entanglement, and we use it to analyze the entanglement of the nearest-neighbor spins, which can be calculated by [86,87]

$$C = \max[0, \sqrt{\lambda_1} - \sqrt{\lambda_2} - \sqrt{\lambda_3} - \sqrt{\lambda_4}], \quad (25)$$

where λ_j ($j = 1, 2, 3, 4$), in decreasing order, are eigenvalues of the non-Hermitian matrix $R = \rho_{l,l+1} \tilde{\rho}_{l,l+1}^*$. Here $\rho_{l,l+1}$ is the reduced density matrix by tracing over all spins in the ground state except the nearest-neighbor spins σ_l and σ_{l+1} [88,89], and it can be written as

$$\rho_{l,l+1} = \begin{pmatrix} a_{11} & 0 & 0 & a_{14} \\ 0 & a_{22} & a_{23} & 0 \\ 0 & a_{32} & a_{33} & 0 \\ a_{41} & 0 & 0 & a_{44} \end{pmatrix}, \quad (26)$$

where

$$a_{11} = \frac{1}{4}M_l + \frac{1}{4}M_{l+1} + \frac{1}{4}\langle \sigma_l^z \sigma_{l+1}^z \rangle + \frac{1}{4}, \quad (27a)$$

$$a_{22} = \frac{1}{4}M_l - \frac{1}{4}M_{l+1} - \frac{1}{4}\langle \sigma_l^z \sigma_{l+1}^z \rangle + \frac{1}{4}, \quad (27b)$$

$$a_{33} = -\frac{1}{4}M_l + \frac{1}{4}M_{l+1} - \frac{1}{4}\langle \sigma_l^z \sigma_{l+1}^z \rangle + \frac{1}{4}, \quad (27c)$$

$$a_{44} = -\frac{1}{4}M_l - \frac{1}{4}M_{l+1} + \frac{1}{4}\langle \sigma_l^z \sigma_{l+1}^z \rangle + \frac{1}{4}, \quad (27d)$$

$$a_{23} = a_{32} = \frac{1}{4}\langle \sigma_l^x \sigma_{l+1}^x \rangle + \frac{1}{4}\langle \sigma_l^y \sigma_{l+1}^y \rangle, \quad (27e)$$

$$a_{14} = \frac{1}{4}\langle \sigma_l^x \sigma_{l+1}^x \rangle - \frac{1}{4}i\langle \sigma_l^x \sigma_{l+1}^y \rangle - \frac{1}{4}i\langle \sigma_l^y \sigma_{l+1}^x \rangle - \frac{1}{4}\langle \sigma_l^y \sigma_{l+1}^y \rangle, \quad (27f)$$

$$a_{41} = \frac{1}{4}\langle \sigma_l^x \sigma_{l+1}^x \rangle + \frac{1}{4}i\langle \sigma_l^x \sigma_{l+1}^y \rangle + \frac{1}{4}i\langle \sigma_l^y \sigma_{l+1}^x \rangle - \frac{1}{4}\langle \sigma_l^y \sigma_{l+1}^y \rangle. \quad (27g)$$

$\tilde{\rho}_{l,l+1} = (\sigma^y \otimes \sigma^y) \rho_{l,l+1}^* (\sigma^y \otimes \sigma^y)$ is the corresponding spin-flipped density matrix, where $\rho_{l,l+1}^*$ is the complex conjugate of $\rho_{l,l+1}$.

Based on Eq. (25), we calculate the concurrence C in the \mathcal{RT} -symmetric and \mathcal{RT} -broken phases, and the results are given in Fig. 7. The variations of C with γ for different values of h are shown in Fig. 7(a). When $0 < h < 1$, C rapidly decreases to zero as γ increases; when $h > 1$, it first increases to a maximum and then decreases to zero, indicating that the crossover behavior of concurrence is prominent. Additionally, the concurrence reaches its maximum at EP and increases with h_c or γ_c . In the special case of $\gamma = 0$, C decreases with the increase of h ; this is because the spins are magnetized as the magnetic field increases, which breaks the entanglement between two spins. Meanwhile, $\partial C / \partial \gamma$ is nonanalytic at EP [see Fig. 7(b)], which indicates that the entanglement can reflect the phase transition from the \mathcal{RT} -symmetric phase to the broken one in this system.

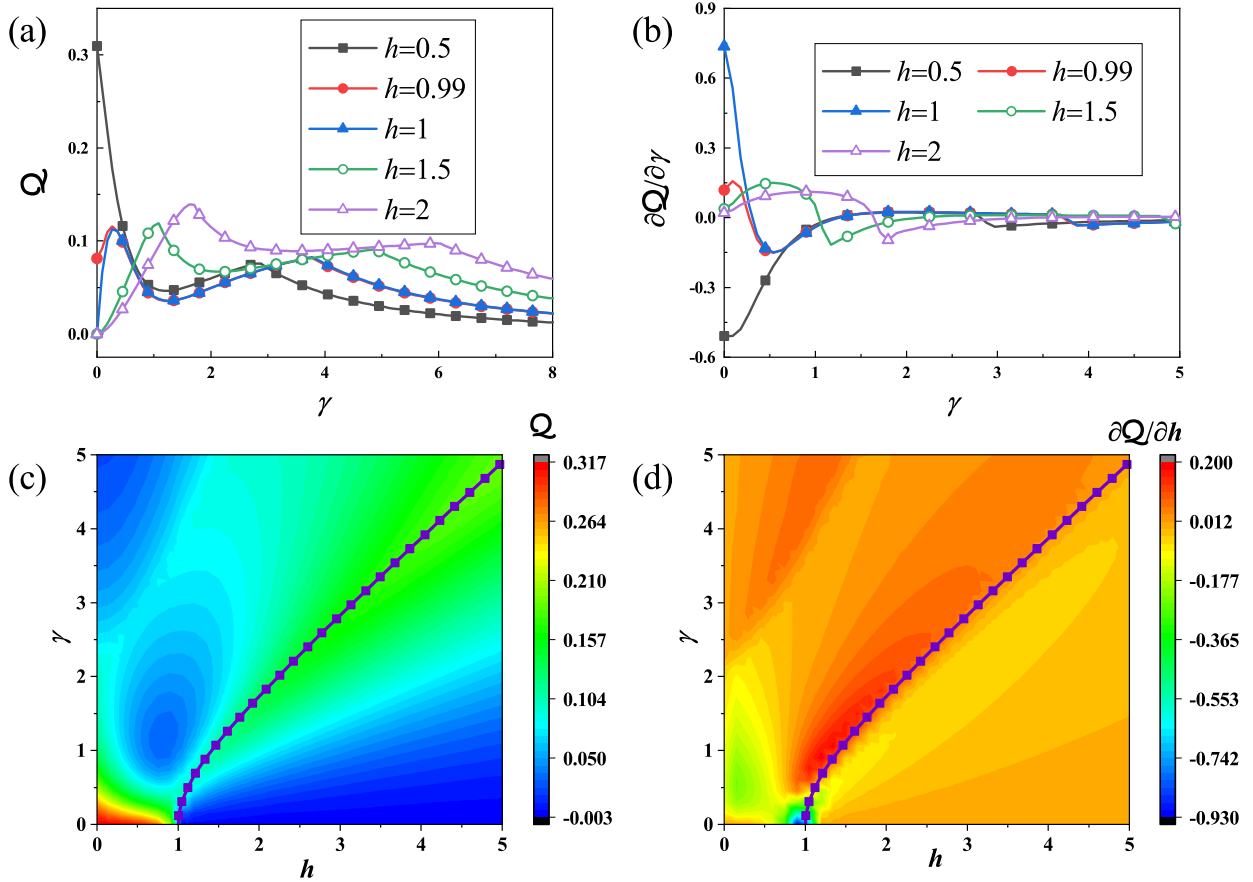


FIG. 8. Quantum discord and its derivative with respect to γ and h . (a) Q oscillates and decreases with γ . (b) $\partial Q / \partial \gamma$ is nonanalytic at EP. (c) Q exists in a wider range than concurrence, and its maximum also appears at the phase boundary. (d) $\partial Q / \partial h$ is nonanalytic at the phase boundary.

To better analyze the crossover behaviors of concurrence in different phases, we discuss the influences of γ and h on C in a contour plot [see Fig. 7(c)]. When h is a certain value, it is shown that C is positively correlated with γ in the \mathcal{RT} -symmetric phase, which is opposite to that in the broken one. For the effects of h , C exhibits a negative correlation with h in the symmetric phase; in the broken one, the variation of C is not monotonic, which shows that it is also negatively connected with h when $0 < h < 1$, while opposite to the case of $1 < h < h_c$. Furthermore, we find that the larger γ or h will weaken C , and the maximum value of C always emerges at the phase boundary where the competition is intense (including the segment for $\gamma = 0$, $0 < h < 1$). In Fig. 7(d), $\partial C / \partial h$ decreases abnormally when crossing from the broken phase to the symmetric one, especially in the case in which γ is relatively small, which corresponds to a junction of the Hermitian region ($\gamma = 0$), the \mathcal{RT} -symmetric phase and the broken one.

B. Ground-state quantum discord

We have identified that entanglement is closely connected to the phase transition of this non-Hermitian XY model. Quantum discord [90,91], a type of quantum correlation with more quantum information than entanglement, has been considered as a sign of a quantum phase transition [92–98]. We next calculate it and discuss its crossover behavior at EP.

Quantum discord can be obtained through the equation

$$\mathcal{Q}(\rho) = \mathcal{I}(\rho) - \mathcal{C}(\rho), \quad (28)$$

in which $\mathcal{I}(\rho)$ and $\mathcal{C}(\rho)$ are quantum mutual information and classical correlation, respectively. Since the calculation process is relatively complicated, we will not go into details.

Figure 8 shows the numerical results (see the detailed calculation process in Ref. [99]) of the quantum discord Q between nearest-neighbor spins in relation to γ and h . From Fig. 8(a) one can find that the behaviors of Q are identical to those of concurrence when $\gamma = 0$; Q oscillates and decreases with γ for a certain h when $\gamma > 0$. Compared with entanglement, it is obvious that Q exists in a wider parameter range (Q still exists when γ is very large). The overall distribution of Q with γ and h is shown in Fig. 8(c). In the symmetric phase, γ and h have opposite effects on Q , while its distribution is relatively complicated in the broken one. Furthermore, the crossover behavior of Q is also evident, which shows that its variations with γ (or h) are opposite on both sides of the phase boundary. We also find that the maximum of Q also appears at EP, and $\partial Q / \partial \gamma$ as well as $\partial Q / \partial h$ are also nonanalytic at EP [see Figs. 8(b) and 8(d)], which has similar phenomena to entanglement.

We emphasize that the ground state considered in this paper differs from the steady state of a dissipative system. For a dissipative system described by the master equation, the

dissipation process tends to destroy quantum information and coherence, resulting in the properties of steady states similar to those of a thermal equilibrium system or one at finite temperature [100–103]. The quantum phase transition describes a sudden change of the ground state by tuning parameters and usually occurs when the energy gap goes to zero. A significant aspect of the non-Hermitian XY model with \mathcal{RT} symmetry is the presence of EP, which separates the \mathcal{RT} -symmetric phase from the broken one. Additionally, one can find that the energy gap coincidentally closes at EP. As a result, the phase transition at EP is quantum and it can be well characterized by GSED and quantum entanglement.

V. CONCLUSION

In this paper, we have studied the ground-state energy density, magnetization, correlation functions, quantum entanglement, and correlation of a non-Hermitian spin-1/2 XY model and focused on the effects of the non-Hermitian parameter γ and external magnetic field h on these physical quantities in \mathcal{RT} -symmetric and \mathcal{RT} -broken phases as well as their crossover behaviors at EP. It is found that the magnetization decays faster with γ in the symmetric region than in the broken one, and declines rapidly at EP. For GSED, when $\gamma > 0$, it decreases linearly with h , while it bifurcates when $\gamma = 0$. By calculating GSED and its derivatives, a second-order phase transition caused by symmetry breaking is confirmed,

and it can be further demonstrated by the magnetization and quantum entanglement, etc. The numerical result of the correlation function is quite interesting, which shows that there is quasi-long-range order in the \mathcal{RT} -broken phase; besides, the exponential decay of it in the symmetric phase implies that the phase has paramagnetic properties. We also find that the crossover behavior of quantum entanglement is obvious, which shows that its variations with γ are opposite before and after crossing the phase boundary, and its maximum always appears at the phase boundary. Overall, the existence of γ makes the behaviors of the above physical quantities unusual, which is actually caused by the competition between γ and h , especially at EP; the competition is so intense that it drives the appearance of the maximum or a sharp change for the above physical quantities.

ACKNOWLEDGMENTS

This work is supported by the National Natural Science Foundation of China under Grants No. 11675090 and No. 11905095, and Shandong Provincial Natural Science Foundation, China, under Grant No. ZR2022MA041. C.M. would like to thank X. Zhang for fruitful discussions and useful comments.

C.M. and Y.L. contributed equally to this work.

-
- [1] N. Moiseyev, *Non-Hermitian Quantum Mechanics* (Cambridge University Press, Cambridge, 2011).
 - [2] Y. Ashida, Z. Gong, and M. Ueda, Non-Hermitian physics, *Adv. Phys.* **69**, 249 (2020).
 - [3] A. J. Daley, Quantum trajectories and open many-body quantum systems, *Adv. Phys.* **63**, 77 (2014).
 - [4] J. Dalibard, Y. Castin, and K. Mølmer, Wave-function approach to dissipative processes in quantum optics, *Phys. Rev. Lett.* **68**, 580 (1992).
 - [5] T. E. Lee and C.-K. Chan, Heralded magnetism in non-Hermitian atomic systems, *Phys. Rev. X* **4**, 041001 (2014).
 - [6] T. E. Lee, F. Reiter, and N. Moiseyev, Entanglement and spin squeezing in non-Hermitian phase transitions, *Phys. Rev. Lett.* **113**, 250401 (2014).
 - [7] Y. Ashida, S. Furukawa, and M. Ueda, Quantum critical behavior influenced by measurement backaction in ultracold gases, *Phys. Rev. A* **94**, 053615 (2016).
 - [8] Y. Ashida, S. Furukawa, and M. Ueda, Parity-time-symmetric quantum critical phenomena, *Nat. Commun.* **8**, 15791 (2017).
 - [9] M. Naghiloo, M. Abbasi, Y. N. Joglekar, and K. W. Murch, Quantum state tomography across the exceptional point in a single dissipative qubit, *Nat. Phys.* **15**, 1232 (2019).
 - [10] C. M. Bender and S. Boettcher, Real spectra in non-Hermitian Hamiltonians having \mathcal{PT} symmetry, *Phys. Rev. Lett.* **80**, 5243 (1998).
 - [11] C. Li, G. Zhang, X. Z. Zhang, and Z. Song, Conventional quantum phase transition driven by a complex parameter in a non-Hermitian \mathcal{PT} -symmetric Ising model, *Phys. Rev. A* **90**, 012103 (2014).
 - [12] C. Li and Z. Song, Generation of Bell, W , and Greenberger-Horne-Zeilinger states via exceptional points in non-Hermitian quantum spin systems, *Phys. Rev. A* **91**, 062104 (2015).
 - [13] C. Li, G. Zhang, and Z. Song, Chern number in Ising models with spatially modulated real and complex fields, *Phys. Rev. A* **94**, 052113 (2016).
 - [14] X. Turkeshi and M. Schiró, Entanglement and correlation spreading in non-Hermitian spin chains, *Phys. Rev. B* **107**, L020403 (2023).
 - [15] F. Bagarello, M. Lattuca, R. Passante, L. Rizzuto, and S. Spagnolo, Non-Hermitian Hamiltonian for a modulated Jaynes-Cummings model with \mathcal{PT} symmetry, *Phys. Rev. A* **91**, 042134 (2015).
 - [16] J. A. S. Lourenço, R. L. Eneias, and R. G. Pereira, Kondo effect in a \mathcal{PT} -symmetric non-Hermitian Hamiltonian, *Phys. Rev. B* **98**, 085126 (2018).
 - [17] A. P. Acharya, A. Chakrabarty, D. K. Sahu, and S. Datta, Localization, \mathcal{PT} -symmetry breaking, and topological transitions in non-Hermitian quasicrystals, *Phys. Rev. B* **105**, 014202 (2022).
 - [18] Q. Du, K. Cao, and S.-P. Kou, Physics of \mathcal{PT} -symmetric quantum systems at finite temperatures, *Phys. Rev. A* **106**, 032206 (2022).
 - [19] A. Guo, G. J. Salamo, D. Duchesne, R. Morandotti, M. Volatier-Ravat, V. Aimez, G. A. Siviloglou, and D. N. Christodoulides, Observation of \mathcal{PT} -symmetry breaking in complex optical potentials, *Phys. Rev. Lett.* **103**, 093902 (2009).
 - [20] S. Weimann, M. Kremer, Y. Plotnik, Y. Lumer, S. Nolte, K. G. Makris, M. Segev, M. C. Rechtsman, and A. Szameit, Topologically protected bound states in photonic parity-time-symmetric crystals, *Nat. Mater.* **16**, 433 (2017).

- [21] R. El-Ganainy, K. G. Makris, M. Khajavikhan, Z. H. Musslimani, S. Rotter, and D. N. Christodoulides, Non-Hermitian physics and \mathcal{PT} symmetry, *Nat. Phys.* **14**, 11 (2018).
- [22] Y. Xing, L. Qi, J. Cao, D. Wang, C. Bai, H. Wang, A. Zhu, and S. Zhang, Spontaneous \mathcal{PT} -symmetry breaking in non-Hermitian coupled-cavity array, *Phys. Rev. A* **96**, 043810 (2017).
- [23] Y. Xue, C. Hang, Y. He, Z. Bai, Y. Jiao, G. Huang, J. Zhao, and S. Jia, Experimental observation of partial parity-time symmetry and its phase transition with a laser-driven cesium atomic gas, *Phys. Rev. A* **105**, 053516 (2022).
- [24] Y. Wu, W. Liu, J. Geng, X. Song, X. Ye, C.-K. Duan, X. Rong, and J. Du, Observation of parity-time symmetry breaking in a single-spin system, *Science* **364**, 878 (2019).
- [25] A. Regensburger, C. Bersch, M. Miri, G. Onishchukov, D. N. Christodoulides, and U. Peschel, Parity-time synthetic photonic lattices, *Nature (London)* **488**, 167 (2012).
- [26] T. E. Lee and Y. N. Joglekar, \mathcal{PT} -symmetric Rabi model: Perturbation theory, *Phys. Rev. A* **92**, 042103 (2015).
- [27] J. Li, A. K. Harter, J. Liu, L. Melo, Y. N. Joglekar, and L. Luo, Observation of parity-time symmetry breaking transitions in a dissipative Floquet system of ultracold atoms, *Nat. Commun.* **10**, 855 (2019).
- [28] G. L. Giorgi, Spontaneous \mathcal{PT} symmetry breaking and quantum phase transitions in dimerized spin chains, *Phys. Rev. B* **82**, 052404 (2010).
- [29] L. Amico, R. Fazio, A. Osterloh, and V. Vedral, Entanglement in many-body systems, *Rev. Mod. Phys.* **80**, 517 (2008).
- [30] J. Eisert, M. Cramer, and M. B. Plenio, Colloquium: Area laws for the entanglement entropy, *Rev. Mod. Phys.* **82**, 277 (2010).
- [31] T. Nishioka, Entanglement entropy: Holography and renormalization group, *Rev. Mod. Phys.* **90**, 035007 (2018).
- [32] R. Horodecki, P. Horodecki, M. Horodecki, and K. Horodecki, Quantum entanglement, *Rev. Mod. Phys.* **81**, 865 (2009).
- [33] N. Gigena, M. Di Tullio, and R. Rossignoli, Many-body entanglement in fermion systems, *Phys. Rev. A* **103**, 052424 (2021).
- [34] X.-X. Xu, Enhancing quantum entanglement and quantum teleportation for two-mode squeezed vacuum state by local quantum-optical catalysis, *Phys. Rev. A* **92**, 012318 (2015).
- [35] X.-M. Hu, Y. Guo, B.-H. Liu, Y.-F. Huang, C.-F. Li, and G.-C. Guo, Beating the channel capacity limit for superdense coding with entangled ququarts, *Sci. Adv.* **4**, eaat9304 (2018).
- [36] S. Wehner, D. Elkouss, and R. Hanson, Quantum internet: A vision for the road ahead, *Science* **362**, eaam9288 (2018).
- [37] G. Gordon and G. Rigolin, Generalized quantum telecloning, *Eur. Phys. J. D* **45**, 347 (2007).
- [38] M. C. Arnesen, S. Bose, and V. Vedral, Natural thermal and magnetic entanglement in the 1D Heisenberg model, *Phys. Rev. Lett.* **87**, 017901 (2001).
- [39] M. Kargarian, R. Jafari, and A. Langari, Dzyaloshinskii-Moriya interaction and anisotropy effects on the entanglement of the Heisenberg model, *Phys. Rev. A* **79**, 042319 (2009).
- [40] F.-W. Ma, S.-X. Liu, and X.-M. Kong, Quantum entanglement and quantum phase transition in the XY model with staggered Dzyaloshinskii-Moriya interaction, *Phys. Rev. A* **84**, 042302 (2011).
- [41] E. Mehran, S. Mahdavi, and R. Jafari, Induced effects of the Dzyaloshinskii-Moriya interaction on the thermal entanglement in spin-1/2 Heisenberg chains, *Phys. Rev. A* **89**, 042306 (2014).
- [42] A. Osterloh, L. Amico, G. Falci, and R. Fazio, Scaling of entanglement close to a quantum phase transition, *Nature (London)* **416**, 608 (2002).
- [43] T. J. Osborne and M. A. Nielsen, Entanglement in a simple quantum phase transition, *Phys. Rev. A* **66**, 032110 (2002).
- [44] L.-A. Wu, M. S. Sarandy, and D. A. Lidar, Quantum phase transitions and bipartite entanglement, *Phys. Rev. Lett.* **93**, 250404 (2004).
- [45] J.-M. Cai, Z.-W. Zhou, and G.-C. Guo, Robustness of entanglement as a signature of quantum phase transitions, *Phys. Lett. A* **352**, 196 (2006).
- [46] T. R. de Oliveira, G. Rigolin, and M. C. de Oliveira, Genuine multipartite entanglement in quantum phase transitions, *Phys. Rev. A* **73**, 010305(R) (2006).
- [47] T. R. de Oliveira, G. Rigolin, M. C. de Oliveira, and E. Miranda, Multipartite entanglement signature of quantum phase transitions, *Phys. Rev. Lett.* **97**, 170401 (2006).
- [48] T. R. de Oliveira, G. Rigolin, M. C. de Oliveira, and E. Miranda, Symmetry-breaking effects upon bipartite and multipartite entanglement in the XY model, *Phys. Rev. A* **77**, 032325 (2008).
- [49] M. Kargarian, R. Jafari, and A. Langari, Renormalization of entanglement in the anisotropic Heisenberg (XXZ) model, *Phys. Rev. A* **77**, 032346 (2008).
- [50] R. Jafari, M. Kargarian, A. Langari, and M. Siahatgar, Phase diagram and entanglement of the Ising model with Dzyaloshinskii-Moriya interaction, *Phys. Rev. B* **78**, 214414 (2008).
- [51] L. Gálisová, Insight into ground-state spin arrangement and bipartite entanglement of the polymeric coordination compound $[\text{Dy}_2\text{Cu}_2]_n$ through the symmetric spin-1/2 Ising-Heisenberg orthogonal-dimer chain, *J. Magn. Magn. Mater.* **561**, 169721 (2022).
- [52] P.-Y. Chang, J.-S. You, X. Wen, and S. Ryu, Entanglement spectrum and entropy in topological non-Hermitian systems and nonunitary conformal field theory, *Phys. Rev. Res.* **2**, 033069 (2020).
- [53] L. Herviou, N. Regnault, and J. H. Bardarson, Entanglement spectrum and symmetries in non-Hermitian fermionic non-interacting models, *SciPost Phys.* **7**, 069 (2019).
- [54] E. Lee, H. Lee, and B.-J. Yang, Many-body approach to non-Hermitian physics in fermionic systems, *Phys. Rev. B* **101**, 121109(R) (2020).
- [55] Á. Bácsi and B. Dóra, Dynamics of entanglement after exceptional quantum quench, *Phys. Rev. B* **103**, 085137 (2021).
- [56] E. Lieb, T. Schultz, and D. Mattis, Two soluble models of an antiferromagnetic chain, *Ann. Phys.* **16**, 407 (1961).
- [57] P. Pfeuty, The one-dimensional Ising model with a transverse field, *Ann. Phys.* **57**, 79 (1970).
- [58] E. Barouch, B. M. McCoy, and M. Mattis, Statistical mechanics of the XY model. I, *Phys. Rev. A* **2**, 1075 (1970).
- [59] B.-Q. Jin and V. E. Korepin, Quantum spin chain, Toeplitz determinants and the Fisher-Hartwig conjecture, *J. Stat. Phys.* **116**, 79 (2004).
- [60] F. Iglói and R. Juhász, Exact relationship between the entanglement entropies of XY and quantum Ising chains, *Europhys. Lett.* **81**, 57003 (2008).

- [61] B.-Q. Liu, B. Shao, J.-G. Li, J. Zou, and L.-A. Wu, Quantum and classical correlations in the one-dimensional XY model with Dzyaloshinskii-Moriya interaction, *Phys. Rev. A* **83**, 052112 (2011).
- [62] D. Sadhukhan, R. Prabhu, A. Sen (De), and U. Sen, Quantum correlations in quenched disordered spin models: Enhanced order from disorder by thermal fluctuations, *Phys. Rev. E* **93**, 032115 (2016).
- [63] F. Mofidnakhai, F. K. Fumani, S. Mahdaviifar, and J. Vahedi, Quantum correlations in anisotropic XY-spin chains in a transverse magnetic field, *Phase Transit.* **91**, 1256 (2018).
- [64] R. Jafari and A. Akbari, Dynamics of quantum coherence and quantum Fisher information after a sudden quench, *Phys. Rev. A* **101**, 062105 (2020).
- [65] M. Kenzelmann, R. Coldea, D. A. Tennant, D. Visser, M. Hofmann, P. Smeibidl, and Z. Tylczynski, Order-to-disorder transition in the XY-like quantum magnet Cs_2CoCl_4 induced by noncommuting applied fields, *Phys. Rev. B* **65**, 144432 (2002).
- [66] P. Babkevich, M. Jeong, Y. Matsumoto, I. Kovacevic, A. Finco, R. Toft-Petersen, C. Ritter, M. Måsson, S. Nakatsuji, and H. M. Rønnow, Dimensional reduction in quantum dipolar antiferromagnets, *Phys. Rev. Lett.* **116**, 197202 (2016).
- [67] L. G. C. Lakkaraju and A. Sen(De), Detection of an unbroken phase of a non-Hermitian system via a Hermitian factorization surface, *Phys. Rev. A* **104**, 052222 (2021).
- [68] Z. Guo, X. Yu, X. Hu, and Z. Li, Emergent phase transitions in a cluster Ising model with dissipation, *Phys. Rev. A* **105**, 053311 (2022).
- [69] X. Z. Zhang and Z. Song, Non-Hermitian anisotropic XY model with intrinsic rotation-time-reversal symmetry, *Phys. Rev. A* **87**, 012114 (2013).
- [70] S. Nixon and J. Yang, All-real spectra in optical systems with arbitrary gain-and-loss distributions, *Phys. Rev. A* **93**, 031802(R) (2016).
- [71] L. Feng, R. El-Ganainy, and L. Ge, Non-Hermitian photonics based on parity-time symmetry, *Nat. Photonics* **11**, 752 (2017).
- [72] L. Ding, K. Shi, Q. Zhang, D. Shen, X. Zhang, and W. Zhang, Experimental determination of \mathcal{PT} -symmetric exceptional points in a single trapped ion, *Phys. Rev. Lett.* **126**, 083604 (2021).
- [73] A. Honma, D. Takane, S. Souma, Y. Wang, K. Nakayama, M. Kitamura, K. Horiba, H. Kumigashira, T. Takahashi, Y. Ando, and T. Sato, Unusual surface states associated with \mathcal{PT} -symmetry breaking and antiferromagnetic band folding in NdSb, *Phys. Rev. B* **108**, 115118 (2023).
- [74] T. Shui, W. Yang, S. Liu, and L. Li, Asymmetric diffraction by atomic gratings with optical \mathcal{PT} symmetry in the Raman-Nath regime, *Phys. Rev. A* **97**, 033819 (2018).
- [75] C. Hang and G. Huang, Parity-time symmetry along with nonlocal optical solitons and their active controls in a Rydberg atomic gas, *Phys. Rev. A* **98**, 043840 (2018).
- [76] Z. Zhou and Z. Yu, Interaction effects on the \mathcal{PT} -symmetry-breaking transition in atomic gases, *Phys. Rev. A* **99**, 043412 (2019).
- [77] C. Hang, W. Li, and G. Huang, Nonlinear light diffraction by electromagnetically induced gratings with \mathcal{PT} symmetry in a Rydberg atomic gas, *Phys. Rev. A* **100**, 043807 (2019).
- [78] A. Biella, F. Storme, J. Lebreuilly, D. Rossini, R. Fazio, I. Carusotto, and C. Ciuti, Phase diagram of incoherently driven strongly correlated photonic lattices, *Phys. Rev. A* **96**, 023839 (2017).
- [79] M. Biondi, G. Blatter, H. E. Türeci, and S. Schmidt, Nonequilibrium gas-liquid transition in the driven-dissipative photonic lattice, *Phys. Rev. A* **96**, 043809 (2017).
- [80] N. Matsumoto, K. Kawabata, Y. Ashida, S. Furukawa, and M. Ueda, Continuous phase transition without gap closing in non-Hermitian quantum many-body systems, *Phys. Rev. Lett.* **125**, 260601 (2020).
- [81] D. P. Pires and T. Macrì, Probing phase transitions in non-Hermitian systems with multiple quantum coherences, *Phys. Rev. B* **104**, 155141 (2021).
- [82] S. Suzuki, J.-I. Inoue, and B. K. Chakrabarti, *Quantum Ising Phases and Transitions in Transverse Ising Models* (Springer-Verlag, Berlin, 2013).
- [83] J. E. Bunder and R. H. McKenzie, Effect of disorder on quantum phase transitions in anisotropic XY spin chains in a transverse field, *Phys. Rev. B* **60**, 344 (1999).
- [84] R. J. Elliott, P. Pfeuty, and C. Wood, Ising model with a transverse field, *Phys. Rev. Lett.* **25**, 443 (1970).
- [85] E. Barouch and B. M. McCoy, Statistical mechanics of the XY model. II. Spin-correlation functions, *Phys. Rev. A* **3**, 786 (1971).
- [86] S. Hill and W. K. Wootters, Entanglement of a pair of quantum bits, *Phys. Rev. Lett.* **78**, 5022 (1997).
- [87] W. K. Wootters, Entanglement of formation of an arbitrary state of two qubits, *Phys. Rev. Lett.* **80**, 2245 (1998).
- [88] S.-J. Gu, C.-P. Sun, and H.-Q. Lin, Universal role of correlation entropy in critical phenomena, *J. Phys. A: Math. Theor.* **41**, 025002 (2008).
- [89] A. Dutta, G. Aeppli, B. K. Chakrabarti, U. Divakaran, T. F. Rosenbaum, and D. Sen, *Quantum Phase Transitions in Transverse Field Spin Models* (Cambridge University Press, Cambridge, 2015).
- [90] H. Ollivier and W. H. Zurek, Quantum discord: A measure of the quantumness of correlations, *Phys. Rev. Lett.* **88**, 017901 (2001).
- [91] L. Henderson and V. Vedral, Classical, quantum and total correlations, *J. Phys. A* **34**, 6899 (2001).
- [92] R. Dillenschneider, Quantum discord and quantum phase transition in spin chains, *Phys. Rev. B* **78**, 224413 (2008).
- [93] M. S. Sarandy, Classical correlation and quantum discord in critical systems, *Phys. Rev. A* **80**, 022108 (2009).
- [94] T. Werlang and G. Rigolin, Thermal and magnetic quantum discord in Heisenberg models, *Phys. Rev. A* **81**, 044101 (2010).
- [95] T. Werlang, C. Trippe, G. A. P. Ribeiro, and G. Rigolin, Quantum correlations in spin chains at finite temperatures and quantum phase transitions, *Phys. Rev. Lett.* **105**, 095702 (2010).
- [96] T. Werlang, G. A. P. Ribeiro, and G. Rigolin, Spotlighting quantum critical points via quantum correlations at finite temperatures, *Phys. Rev. A* **83**, 062334 (2011).
- [97] T. Werlang, G. A. P. Ribeiro, and G. Rigolin, Interplay between quantum phase transitions and the behavior of quantum correlations at finite temperatures, *Int. J. Mod. Phys. B* **27**, 1345032 (2013).
- [98] V. K. Vimal and V. Subrahmanyam, Quantum correlations and entanglement in a Kitaev-type spin chain, *Phys. Rev. A* **98**, 052303 (2018).

- [99] M. Ali, A. R. P. Rau, and G. Alber, Quantum discord for two-qubit X states, *Phys. Rev. A* **81**, 042105 (2010).
- [100] A. Mitra, S. Takei, Y. B. Kim, and A. J. Millis, Nonequilibrium quantum criticality in open electronic systems, *Phys. Rev. Lett.* **97**, 236808 (2006).
- [101] L. M. Sieberer, S. D. Huber, E. Altman, and S. Diehl, Dynamical critical phenomena in driven-dissipative systems, *Phys. Rev. Lett.* **110**, 195301 (2013).
- [102] R. Rota, F. Minganti, C. Ciuti, and V. Savona, Quantum critical regime in a quadratically driven nonlinear photonic lattice, *Phys. Rev. Lett.* **122**, 110405 (2019).
- [103] W. Verstraelen, D. Huybrechts, T. Roscilde, and M. Wouters, Quantum and classical correlations in open quantum spin lattices via truncated-cumulant trajectories, *PRX Quantum* **4**, 030304 (2023).